Supporting Information for

Slow Electron-Hole Recombination in Lead Iodide Perovskites Does Not Require a Molecular Dipole

Subham Dastidar,[1] Siming Li,[1] Sergey Y. Smolin,[1] Jason B. Baxter,[1] Aaron T. Fafarman[1*]

[1]Department of Chemical and Biological Engineering, Drexel University, 3141 Chestnut Street, Philadelphia, Pennsylvania 19104, United States

AUTHOR INFORMATION

Corresponding author

E-mail: fafarman@drexel.edu

A. Materials and Synthesis

Cesium lead iodide: Cesium lead iodide films were prepared following the method devised by Eperon et al. with certain modifications.[1] An equimolar (0.5 M) solution of cesium iodide (CsI – Acros Organics, 99.999%) and lead Iodide (PbI_2 – Strem Chemicals, 99.999+%) was prepared in anhydrous *N,N*-dimethylformamide (DMF – Acros Organics, 99.8% Extra dry) and left under continuous stirring for two hours at 120°C. The solution was filtered using a 20 nm Anotop filter (Whatman) and continued to stir at 120°C for another 30 minutes before spin coating on a clean pre-heated (120°C) quartz 1" round at 2500 rpm for 1 min. The resulting film was a yellow polymorph of $CsPbI_3$. The yellow to black phase conversion was performed by annealing the thin film at 350°C for 10 min on a hot plate. To maintain the black perovskite phase, the films were removed from the hot plate and quenched rapidly by placing them on top of a metallic plate at room temperature. All the synthesis procedures were performed inside a N_2 filled glove box.

Methylammonium lead iodide: An $MAPbI_{3-x}Cl_x$ control was prepared according to literature procedures.[2,3] Methylammonium iodide (MAI - Sigma-Aldrich, 98%) and lead chloride ($PbCl_2$ - Sigma-Aldrich) were dissolved in DMF at a respective 3:1 molar ratio. The solution was spincast on quartz rounds at 2000 rpm for 1 min, allowed to dry at room temperature for 20 min and then annealed at 90°C for 120 min. All the synthesis procedures were performed inside a N_2 filled glove box.

B. Characterization

Absorption spectroscopy: Transmission spectra for the thin films on quartz rounds were collected using a PerkinElmer LAMBDA 35 UV-vis spectrophotometer. $CsPbI_3$ samples were encapsulated by sealing the sample in a custom built gas-tight cell consisting of a rubber O-ring compressed between two opposing quartz windows, secured inside a lens tube.

Powder X-ray diffraction (XRD): The X-Ray patterns were collected on a Diffractometer (Rigaku Smartlab), using a Cu anode X-ray tube operating at 3 kW; the wavelength CuK_{α} = 0.154 nm. The thin films were prepared on glass microscope slides using the methods mentioned previously and characterized encapsulated underneath a sheet of polyetherimide plastic, sealed with a bead of glue around the edges to act as a moisture barrier.

Scanning electron microscopy (SEM): A Zeiss Supra 50VP microscope was used to collect the micrographs of the samples. The samples were prepared on the conductive side of ITO-coated glass slides using identical methods as depicted earlier and preserved in a N_2 atmosphere before transferring to SEM with brief air exposure before analysis. The characterization was performed at 8 kV working voltage.

Atomic force microscopy (AFM): Film thickness measurements were performed using a Veeco (Bruker) Metrology, Inc., Multimode NanoScope IIId Scanning Probe Microscope System with films prepared on Si-SiO_2 substrates. The films deposited on Si-SiO_2 were scratched using a razor blade, exposing the substrate underneath. The surface roughness RMS of the exposed SiO_2 was 0.7 nm indicating the razor did not gouge the surface. The measured thickness is 240 ± 20 nm (RMS: 22 nm) for $CsPbI_3$ films.

Spectroscopic ellipsometry: Spectroscopic ellipsometry measurements were taken to develop an optical model for $CsPbI_3$ from which an absorption coefficient could be obtained. The films used for transient spectroscopies possessed relatively large crystal grains, which cause problematic scattering for ellipsometry. An alternative synthetic procedure was used to make smaller grained, smoother films, developed by Eperon et al,[1] with slight modification: drops of hydroiodic acid (HI) were added to the solution of CsI and PbI_2 prior to spincasting. These films

were measured with a J.A. Woollam M2000 spectroscopic ellipsometer at incident angles of 50, 60 and 70° over a spectroscopic energy range of 0.8 to 3.4 eV. Corresponding transmission data was collected on the instrument and used to further constrain the model. Simultaneous fitting of variable angle spectroscopic ellipsometry and transmission data was performed using the CompleteEase software package employing a B-spline model to estimate the complex dielectric function (refractive index) for $CsPbI_3$. The absorption coefficients for $CsPbI_3$ at the excitation wavelengths 400 nm, 530 nm and 650 nm are $2.85x10^5$, $0.8x10^5$ and $0.32x10^5$ cm^{-1}, respectively.

Nanosecond – microsecond transient absorption spectroscopy: The long time range transient absorbance (TA) experiments were performed at the Advanced Optical Spectroscopy and Microscopy Facility in the Center for Functional Nanomaterials at Brookhaven National Laboratory (BNL). The measurements were conducted using a spectrometer coupled to a Ti:sapphire amplified laser system (SpectraPhysics Spitfire Pro, 1 kHz repetition rate), described previously.[4] A commercial optical parametric amplifier (LightConversion) was used to generate the excitation light. For probing, the output of a ~700 ps pulse width supercontinuum fiber laser is electronically synchronized to the femtosecond pump pulse, providing sub-nanosecond time resolution. Multiwavelength transient spectra are recorded using dual spectrometers (signal and reference) equipped with fast Si array detectors. Samples were photoexcited with 1.9 eV (650 nm) photons under $1\mu J/cm^2$ pulse power.

Time-resolved terahertz spectroscopy (TRTS): TRTS was performed using a regeneratively amplified Ti:sapphire laser (Coherent Libra HE) operating at 1 kHz repetition rate and 50 fs pulse duration. An optical parametric amplifier (Coherent OPerA Solo) was used to tune excitation energy. Samples were excited with 3.1 eV (400 nm), 2.3 eV (530 nm) and 1.9 eV (650

nm) pump pulses, then probed at various delay times with terahertz radiation generated and detected using ZnTe nonlinear crystals. For average TRTS conductivity measurements, the change in transmission upon chopped photoexcitation was normalized by the nonphotoexcited signal to determine $\Delta E/E$. The pump power was varied from 1 to 200 μJ/cm^2 for power-dependent studies. The films were sealed under nitrogen inside the custom gas-tight cell as described earlier.

C. Measurement of photoconductivity and mobility from terahertz transients

The photo-induced reduction of the terahertz electric field, determined at peak of the terahertz waveform in the time domain, is defined as $\Delta E(t_p)$, where t_p is the pump-probe delay time. The change in amplitude is directly proportional to the sheet photoconductivity, σ_{sheet}, of the thin film according to following equation:[5]

$$\sigma_{sheet}(t_p) = -\left(\frac{\Delta E(t_p)}{E}\right)(n_A + n_B)c\varepsilon_0 \quad (1)$$

where E is the peak magnitude of the terahertz electric field for the non-photoexcited sample; n_A and n_B are the refractive indices of the surrounding materials at terahertz frequencies; c is the speed of light; and ε_0 is the permittivity of the free space.

For our measurement, the pump was incident on the front surface, i.e. n_A represents the refractive index of air = 1. Since the absorption depth of the films, d (estimated as the inverse of the absorbance coefficient of the material at the pump wavelength), is smaller than the thickness of the films when the excitation wavelengths are 400 nm and 530 nm, the material on the other side of the photoexcited region is the unexcited perovskite, i.e. n_B = the refractive index of $CsPbI_3$. For 650 nm excitation, the film thickness is smaller than the absorption depth. Therefore, n_B is equal to the refractive index of the quartz substrate in this case.

The photoexcited charge carrier concentration was determined from the pump pulse energy at the excitation wavelengths. The reflection loss for normal incidence of the pump pulse, caused by the change in refractive index at the interfaces was calculated from the Fresnel equation. The estimated reflection loss is about 25%.

Since TRTS does not distinguish between conductivity arising from electrons and from holes, the reported mobility values are the sum of photoexcited electron and hole mobilities. The carrier mobility is related to photoconductivity through following equation: $\phi\Sigma\mu_i = \sigma_{sheet}/[q \cdot N]$ as explained in the main text.

D. Kinetic modeling of TRTS data

The recombination dynamics of the free charge carrier density, *n*, was modeled following the precedent set by Wehrenfennig *et al.* in studies of $MAPbI_3$.[6] The decay of the population of free carriers is presumed to occur through mono-, bi-, and tri-molecular processes. Considering the diffusion term, the carrier decay can be modeled with a first-principle partial differential equation:

$$\frac{\partial n(x,t)}{\partial t} = D\frac{\partial^2 n(x,t)}{\partial x^2} - k_1 n(x,t) - k_2 n^2(x,t) - k_3 n^3(x,t) \qquad (2)$$

A numerical solution to the partial differential equation was found using finite difference techniques, employing a space domain divided into 500 discrete slabs and the time domain discretization based on the experimental data spacing. The initial carrier density distribution follows a Beer's law distribution:

$$n(x, t = 0) = n_0 \exp(-\alpha x) \qquad (3)$$

Where n_0 is the carrier density at the front surface:

$$n_0 = \frac{I_0(1-R)\alpha}{hc/\lambda} \quad (4)$$

I_0 is the measured fluence at a pump wavelength of λ and R is the reflectivity of the sample at normal incidence. The boundary conditions of no-flux were used:

$$\frac{dn}{dx}\left(x = 0, x = x_{film}\right) = 0 \quad (5)$$

where x_{film} is the thickness of the film.

The solution in the form of $n(x,t)$ was numerically integrated over the film thickness to calculate the photoexcited aerial carrier density, $N(t)$. As mentioned in the main text, the sheet photoconductivity is proportional to the number of excited carriers per unit area, by $\sigma_{\text{sheet}} = \phi \cdot q \cdot N \cdot \Sigma\mu_i$. Therefore, the reduction of the terahertz electric field due to photoexcitation is proportional to the photoexcited aerial density by

$$\frac{\Delta E}{E}(t) = -\left[\frac{\phi q \sum \mu_i}{\varepsilon_0 c(n_A + n_B)}\right] N(t) \quad (6)$$

The value of the bracketed term was fit from the linear, low fluence, region of the terahertz data for each set of data and used to convert aerial carrier density, $N(t)$, to $\frac{\Delta E}{E}$. It was assumed that every photon absorbed generates free charge carriers, i.e. the exciton-carrier branching ratio, ϕ, equals 1. The sum of squares error between the experimental and calculated data was minimized by varying the recombination rate constants.

E. Diffusion length calculation

The diffusion length can be calculated as a function of charge carrier density using following relationship:

$$L_D = \sqrt{\tau(n) * D} \qquad (7)$$

Where, $D = \frac{\mu k_B T}{q}$ is the diffusion coefficient calculated from the estimated mobility value, and $\tau(n)$ is the half-life of the transient absorption decay from a champion film measured at low fluence (Figure 3, main text), such as would be present during solar cell operation.

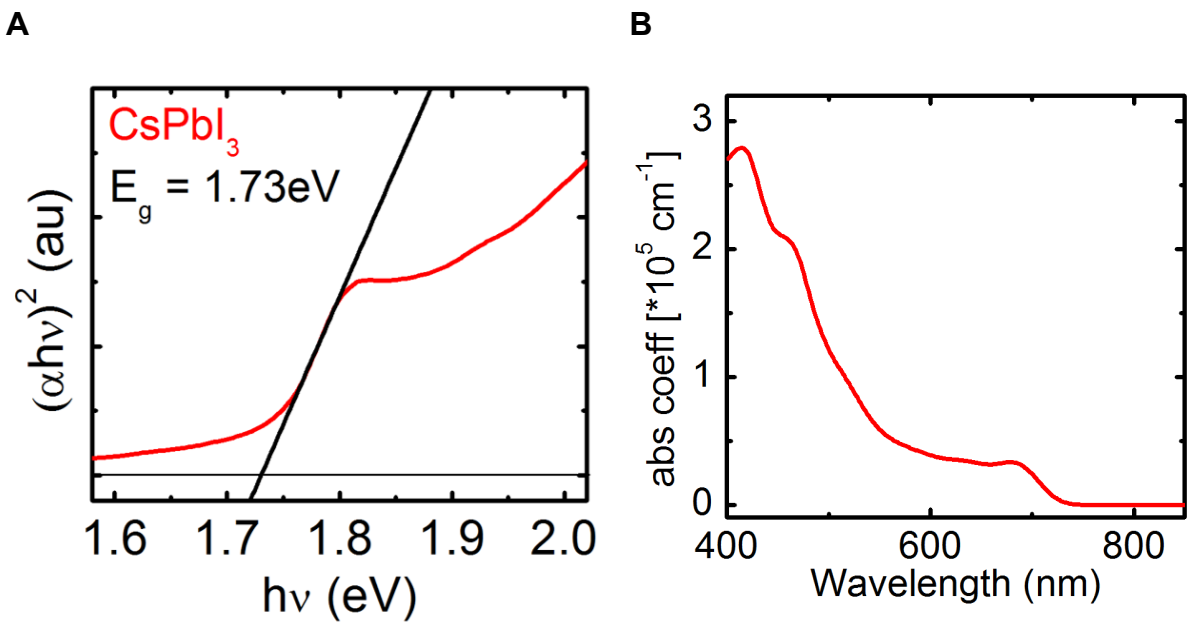

Figure S1. (A) Estimation of bandgap from a Tauc plot of transmission data, assuming a direct bandgap transition. The bandgap evaluated from the x – axis intercept is 1.73 eV. (B) Absorption coefficient of $CsPbI_3$ as obtained from spectroscopic elipsometry.

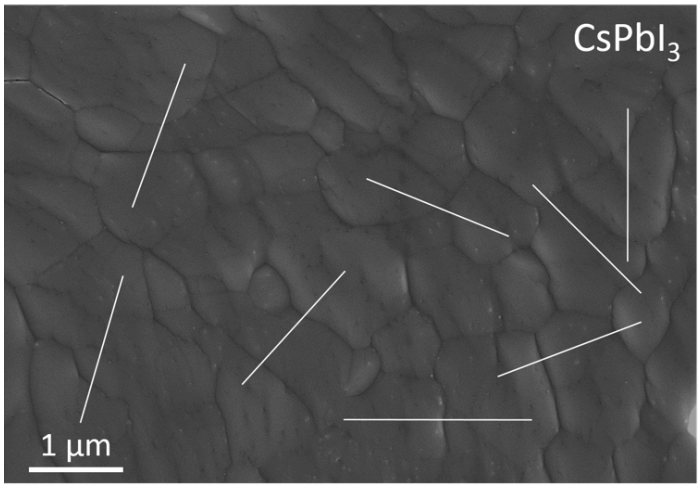

Figure S2. Scanning electron micrograph of thin film of $CsPbI_3$. The mean sizes of the grains were estimated using the intercept method described elsewhere.[7] Multiple lines (here 8 lines of 2 µm length) were drawn across the micrograph and the number of apparent grain boundaries intercepted by each line were tabulated. Dividing total length of the lines (here 16 µm) by the total number of intercepts, provides the mean sizes of the grains. The grain size acquired after averaging for five images is 800 ± 100 nm for $CsPbI_3$.

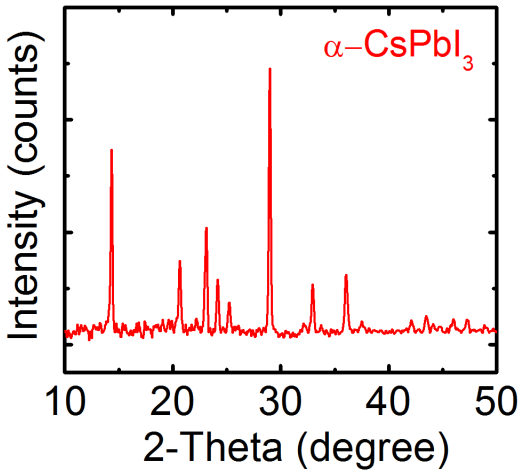

Figure S3. X-Ray diffraction spectrum for a polycrystalline thin film of $CsPbI_3$ (black or 'α' polymorph). The diffraction spectrum confirms $CsPbI_3$ has a cubic structure.

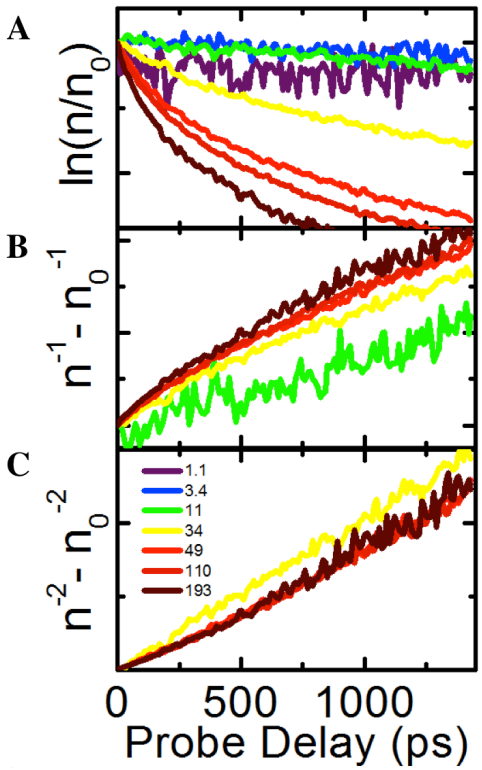

Figure S4. Transient data for 530 nm excitation wavelength, converted into estimated average carrier concentration, *n*, and plotted in functional forms that are linear under pure 1st-, 2nd- or 3rd-order kinetics for A-C, respectively. Fluence values in μJ/cm^2 are indicated for each curve in the inset legend in Panel 3.

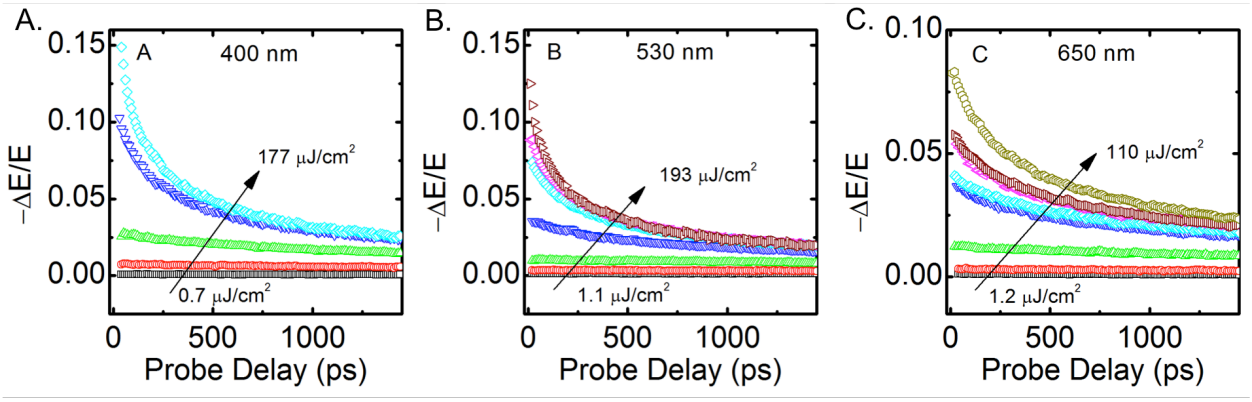

Figure S5. THz transients of $CsPbI_3$ at excitation wavelengths of (A) 400 nm; (B) 530 nm and, (C) 650 nm.

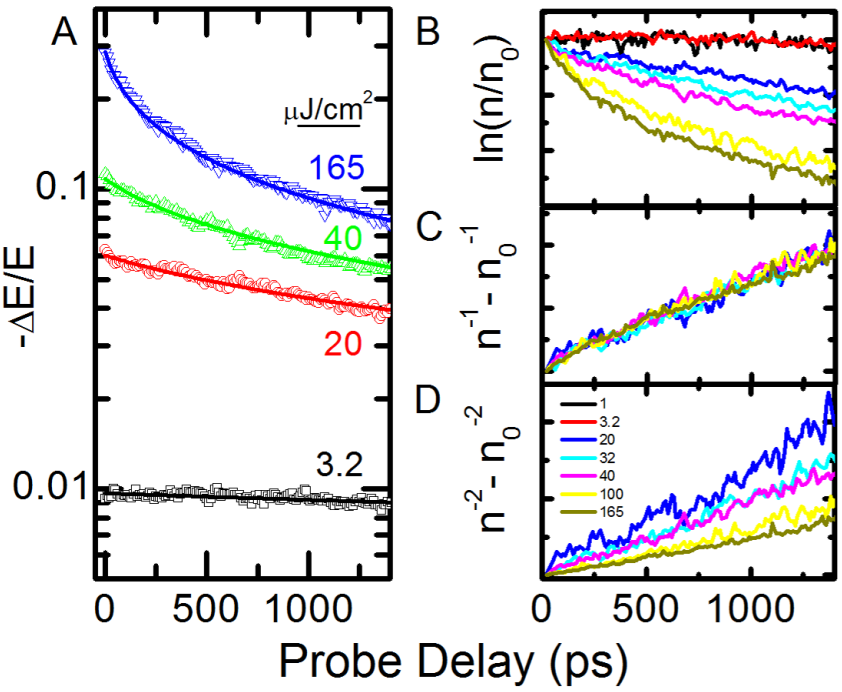

Figure S6. THz transients of $MAPbI_{3-x}Cl_x$ for an excitation wavelength of 550 nm. (A). Transient data are shown as symbols for selected values of the pump fluence (indicated on curve labels). Numerical fits to the data are shown by thin, solid lines. (B-D) Transient data converted into estimated average carrier concentration, *n*, and plotted in functional forms that are linear under pure 1st-, 2nd- or 3rd-order kinetics for B-D, respectively. Transients for all fluence values from 1 to 165 μJ/cm² as indicated in the inset figure legend.

References:

(1) Eperon, G. E.; Paternò, G. M.; Sutton, R. J.; Zampetti, A.; Haghighirad, A. A.; Cacialli, F.; Snaith, H. J. Inorganic Caesium Lead Iodide Perovskite Solar Cells. *J. Mater. Chem. A* **2015**, *3*, 19688–19695.

(2) Lee, M. M.; Teuscher, J.; Miyasaka, T.; Murakami, T. N.; Snaith, H. J. Efficient Hybrid Solar Cells Based on Meso-Superstructured Organometal Halide Perovskites. *Science* **2012**, *338*, 643–647.

(3) deQuilettes, D. W.; Koch, S.; Burke, S.; Paranji, R. K.; Shropshire, A. J.; Ziffer, M. E.; Ginger, D. S. Photoluminescence Lifetimes Exceeding 8 Ms and Quantum Yields Exceeding 30% in Hybrid Perovskite Thin Films by Ligand Passivation. *ACS Energy Lett.* **2016**, *1*, 438–444.

(4) Milleville, C. C.; Pelcher, K. E.; Sfeir, M. Y.; Banerjee, S.; Watson, D. F. Directional Charge Transfer Mediated by Mid-Gap States: A Transient Absorption Spectroscopy Study of CdSe Quantum Dot/β-Pb0.33V2O5 Heterostructures. *J. Phys. Chem. C* **2016**, *120*, 5221–5232.

(5) Nienhuys, H.-K.; Sundström, V. Intrinsic Complications in the Analysis of Optical-Pump, Terahertz Probe Experiments. *Phys. Rev. B* **2005**, *71*, 235110.

(6) Wehrenfennig, C.; Eperon, G. E.; Johnston, M. B.; Snaith, H. J.; Herz, L. M. High Charge Carrier Mobilities and Lifetimes in Organolead Trihalide Perovskites. *Adv. Mater.* **2014**, *26*, 1584–1589.

(7) Hoffman, J. B.; Schleper, A. L.; Kamat, P. V. Transformation of Sintered CsPbBr3 Nanocrystals to Cubic CsPbI3 and Gradient CsPbBrxI3–x through Halide Exchange. *J. Am. Chem. Soc.* **2016**, *138*, 8603–8611.